Improved contrast in dynamic contrast enhanced MRI by combining complex in-phase and opposed-phase data: Simulations and phantom experiment

K-H. Herrmann[1], A. Rauscher[1], W. A. Kaiser[2], J. R. Reichenbach[1]

[1]Medical Physics Group, IDIR, Friedrich-Schiller University, Jena, Germany, [2]IDIR, Friedrich-Schiller University, Jena, Germany

Introduction

Combining complex in-phase (*ip*) and opposed-phase (*op*) images in dynamic contrast enhanced MRI can improve and change the contrast, especially for partially volumed voxels [1,2]. The aim of this work was to investigate possible contrasts generated by different complex combinations of *ip* and *op* data and to verify the calculated and simulated results by phantom experiments.

Methods and Results

For a simple two compartment model the expected native (S_N) and contrast enhanced (CE) signal (S_C) in a voxel containing fat and water is given by:

$$S_N(t) = I_{w_n} e^{i\omega_w t} + I_f e^{i\omega_f t} \quad (1)$$

$$S_C(t) = I_{w_c} e^{i\omega_w t} + I_f e^{i\omega_f t}, \quad (2)$$

where I_{w_n} and I_{w_c} are the native and CE signal from the water fraction and I_f the signal from the fat fraction of the voxel. Assuming a phase of zero for water and inserting appropriate phase terms according to *ip* and *op* conditions, several signal contrasts can be calculated:

$$\left|S_C^{ip}(t)\right| - \left|S_N^{ip}(t)\right| = I_{w_c} - I_{w_n} \quad (3)$$

$$\left|S_C^{ip}(t) + S_C^{op}(t)\right| = 2I_{w_c} \quad (4)$$

$$\left|S_N^{ip}(t) + S_N^{op}(t)\right| = 2I_{w_n} \quad (5)$$

$$\left|S_C^{ip}(t) + S_C^{op}(t)\right| - \left|S_N^{ip}(t) + S_N^{op}(t)\right| = 2(I_{w_c} - I_{w_n}) \quad (6)$$

$$\text{for} \quad I_{w_c} \le I_f: \quad \left|S_C^{ip}(t)\right| - \left|S_C^{op}(t)\right| = 2I_{w_c} \quad (7)$$

$$\left|S_C^{ip}(t) - S_C^{op}(t)\right| = 2I_f. \quad (8)$$

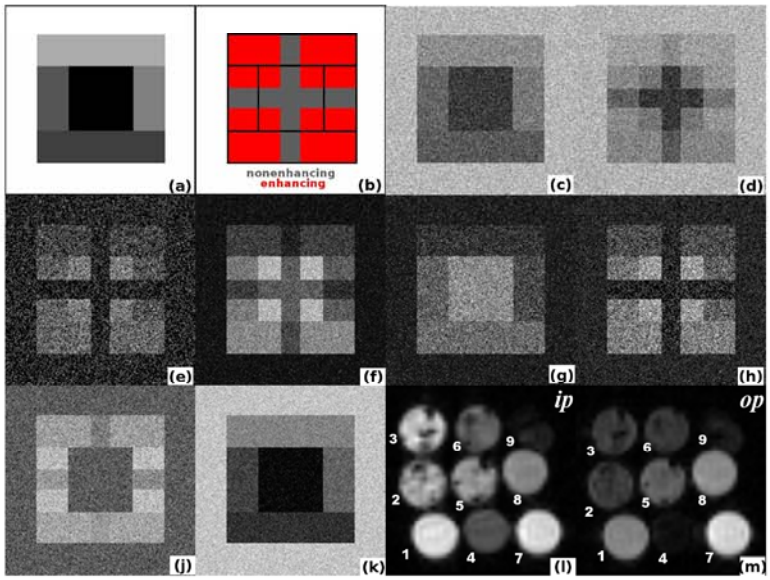

Figure 1: Contrast simulations, all images are windowed individually: **(a)** shows the fat fraction in the voxel (black=0%, white=100%). **(b)** Overlayed on (a), a contast enhancement by a factor f=1.8 is simulated for the water fraction in the red areas, the gray bars and the 100% fat (white) do not enhance. **(c)** native *ip*-image with added complex gaussian noise (SNR of native water ≈ 3.3, fat ≈ 10). **(d)** CE *ip*-image with added complex gaussian noise. **(e)-(k)** Subtractions according to eq. (3)-(8). **(l),(m)** Phantom experiment with cups containing different fat fractions, (l) *ip*, (m) *op*: cup number (1)-(3): CE 30%, 80% and 50% fat content; number (4)-(6): native 30%, 80% and 50% fat; (8): 100% fat; (7) 0% fat CE and (9) native. The contrast agent was 0.8 mmol/l Gd-DTPA in the water fraction.

In comparison to the conventional *ip*-subtraction (eq. (3)), the complex combinations (eq. (4)-(6)) generate a higher signal. To demonstrate that these signal gains do indeed increase image contrast, the contrast between an enhancing and a non-enhancing voxel (Fig. 1b), containing the same partial fat fraction, was calculated where f is the signal enhancement factor due to contrast agent, i.e. $I_{w_c} = fI_{w_n}$: For eq. (3) the contrast is given in eq. (9). Both, the complex addition eq. (4) and the addition/subtraction eq. (6) show a factor 2 higher contrast (eq. (10), (11)).

$$\text{eq. (3)} \Rightarrow I_{w_c} - I_{w_n} = (f-1)I_{w_n} \quad (9)$$

$$\text{eq. (4)} \Rightarrow I_{w_c} - I_{w_n} = \mathbf{2}(f-1)I_{w_n} \quad (10)$$

$$\text{eq. (6)} \Rightarrow I_{w_c} - I_{w_n} = \mathbf{2}(f-1)I_{w_n} \quad (11)$$

For visual assessment a multivoxel simulation was performed with areas of different fat fractions (Fig. 1a). Overlayed on these partial volumed voxels is an enhancement pattern of the water fraction (fat is assumed to not enhance in the presence of Gd-DTPA). Figure 1b details the enhancing (red, f=1.8) and non-enhancing (gray,white) areas. To assess the actual contrast gain, uncorrelated gaussian noise was added to the simulated basic images for the pre- and post-CE *ip* and *op* data (Fig. 1c,d). The resulting images of the various complex image combinations are displayed in Fig.1e-k. Clearly, the complex addition (Fig.1f) has a better contrast compared to the conventional *ip* subtraction (Fig.1e). However, (Fig.1f) still does not display non-enhancing areas (especially the center with 100% water) as black. After subtracting the native complex *ip-op* image (Fig. 1g) from Fig. 1f the contrast remains the same (Fig. 1h), but the non-enhancing areas are displayed as dark as the background. The magnitude *ip-op* subtraction (Fig.1j, [2]) strongly enhances all partial volumed CE areas; however, it is difficult to distinguish them from non-enhancing areas. The fat separation (eq. (8)) is shown in Fig.1k, which reproduces Fig. 1a very well. To verify the contrast gain and fat separation a phantom experiment with a T_1-weighted sequence (TR/TE_1/TE_2/α=7 ms/2.38 ms/4.76 ms/10°) was performed. The images are shown in Fig. 1l and m, the ROI based evaluation of the complex subtractions is summarized in table 1.

Conclusions

Combining *ip* and *op* data opens up a range of different contrast amplifications in comparison to the regular *ip* subtraction (SIP). Especially eq. (4) and the baseline corrected eq.(11) highlight partially volumed enhancing areas (Fig.1f and h). These complex *ip-op*-addition may improve the delineation of lesions by emphasizing the partially volumed lesion boundaries. The fat/water separation given in [1] is certainly more robust but need a dedicated scan. The complex *ip-op* subtraction can at least qualitatively determine the fat signal using a dual-echo sequence with no increase in measuring time and is therefore even possible for dynamic MRI.

Fat content	0%	30%	50%	80%	100%
native IP	26	75	89	134	120
native OP	28	11	46	82	113
CA IP	158	167	174	148	nat. IP
CA OP	164	113	55	51	nat. OP
eq. (3)	132	92	86	13	0
eq. (4)	280	234	200	83	45
eq. (6)	228	184	178	16	0
eq. (8)	97	32	100	173	222

Table 1: Overview of the phantom results, the numbers give the signal intensity. The subtractions were performed by using averaged ROI based complex image data. Where appropriate, the modulus was taken before or after subtraction.

[1] S. B. Reeder, A. R. Pineda, Z. Wen, A. Shimakawa, H. Yu, J. H. Brittain, G. E. Gold, C. H. Beaulieu, and N. J. Pelc. Iterative decomposition of water and fat with echo asymmetry and least-squares estimation (ideal): application with fast spin-echo imaging. *Magn Reson Med.*, 54(3):636–644, 2005.

[2] J. R. Reichenbach, J. Hopfe, A. Rauscher, S. Wurdinger, and W. A. Kaiser. Subtraction on in-phase and opposed-phase images in dynamic mr-mammography (sipop). *J Magn Reson Imaging*,21(5):565-575, 2005.